Nanoscale

PAPER

View Article Online
View Journal | View Issue

Cite this: *Nanoscale*, 2016, **8**, 13445

The role of Rabi splitting tuning in the dynamics of strongly coupled J-aggregates and surface plasmon polaritons in nanohole arrays

Hai Wang,[a,b] Andrea Toma,*[a] Hai-Yu Wang,*[b] Angelo Bozzola,[a] Ermanno Miele,[a] Ali Haddadpour,[c,d] Georgios Veronis,[c,d] Francesco De Angelis,[a] Lei Wang,[b] Qi-Dai Chen,[b] Huai-Liang Xu,[b] Hong-Bo Sun*[b] and Remo Proietti Zaccaria*[a,e]

Received 25th February 2016,
Accepted 13th June 2016

DOI: 10.1039/c6nr01588c

www.rsc.org/nanoscale

We have investigated the influence of Rabi splitting tuning on the dynamics of strongly coupled J-aggregate/surface plasmon polariton systems. In particular, the Rabi splitting was tuned by modifying the J-aggregate molecule concentration while a polaritonic system was provided by a nanostructure formed by holes array in a golden layer. From the periodic and concentration changes we have identified, through numerical and experimental steady-state analyses, the best geometrical configuration for maximizing Rabi splitting, which was then used for transient absorption measurements. It was found that in transient absorption spectra, under upper band excitation, two bleaching peaks appear when a nanostructured polaritonic pattern is used. Importantly, their reciprocal distance increases upon increase of J-aggregate concentration, a result confirmed by steady-state analysis. In a similar manner it was also found that the lifetime of the upper band is intimately related to the coupling strength. In particular, we argue that with strong coupling strength, *i.e.* high J-aggregate concentration, a short lifetime of the upper band has to be expected due to the suppression of the bottleneck effect. This result supports the idea that the dynamics of hybrid systems is profoundly dependent on Rabi splitting.

Introduction

Matter–light interaction is surely one of the most fundamental processes occurring in nature, and the interaction between molecular excitons and surface plasmon polariton (SPP) modes is one of its most effective forms. When the interaction is weak, the wave function of molecules and the SPP modes can be treated as unperturbed, only leading to modification of the spontaneous emission rate. On the other hand, when the interaction is strong enough, upon light irradiation a reversible energy is exchanged between the excitons and SPP modes at a rate faster than their respective damping processes. The result is the formation of a hybrid[1,2] exciton–SPP state: the system is in a strong coupling regime.[3–9] The new state is formed by two energy bands (upper and lower band) separated by an energy value known as the Rabi splitting energy $\hbar\Omega_R$ (Ω_R, the energy exchange rate between the hybrid bands). The hybrid state is characterized by the mixed properties of molecules and SPPs, which is similar to the behaviour of polaritons in an optical microcavity.[10–16] Such an intrinsic peculiarity makes hybrid states interesting for both fundamental research and applications. It has been demonstrated that the strong coupling with organic molecules can display a very large vacuum Rabi splitting (up to 700 meV with SPPs; more than 1 eV in a cavity), comparable to a significant fraction of the molecular transition energy.[13,17,18] The strong modification of the energy levels of the hybrid system has been used to tune chemical reaction rates[19] and the work function of organic materials.[20] In particular, due to the bosonic character of the hybrid states, non-equilibrium Bose–Einstein condensation has been observed at room temperature.[21] From a dynamics perspective, the Rabi oscillations between J-aggregate molecules and SPPs have been recently measured in real time on a 10 fs timescale,[22] the first step towards the realization of next stage nano-plasmonic devices, such as all-optical switches and low threshold nanolasers.[11,23,24] The choice of this kind of molecule is dictated by the need for realizing strong coupling.

[a]*Istituto Italiano di Tecnologia, via Morego 30, 16163 Genova, Italy. E-mail: remo.proietti@iit.it, andrea.toma@iit.it*
[b]*State Key Laboratory on Integrated Optoelectronics, College of Electronic Science and Engineering, Jilin University, Changchun 130012, China. E-mail: hbsun@jlu.edu.cn, haiyu_wang@jlu.edu.cn*
[c]*School of Electrical Engineering and Computer Science, Louisiana State University, Baton Rouge, Louisiana 70803, USA*
[d]*Center for Computation and Technology, Louisiana State University, Baton Rouge, Louisiana 70803, USA*
[e]*Cixi Institute of Biomedical Engineering, Ningbo Institute of Materials Technology and Engineering, Chinese Academy of Sciences, Ningbo 315201, China*

Indeed, according to the definition, strong coupling is achieved if the Rabi splitting is wider than the linewidths of both the SPP mode and the molecule absorption resonance. In this regard, J-aggregates show a narrow absorption band, much narrower than standard dye molecules (such as Rhodamine 6G, Sulforhodamine 101, Rhodamine 800, Nile red and beta-carotene) which instead are characterized by inhomogeneously broad spectra.

In the absence of dissipation, the Rabi splitting energy $\hbar\Omega_R$ (*i.e.* the coupling strength) of an individual two-level oscillator at resonance with the SPP vacuum field $\vec{E}$, is given by:[25]

$$\hbar\Omega_R = 2\vec{E}\cdot\vec{d}\sqrt{n_{ph}+1} = 2\sqrt{\frac{\hbar\omega}{2\varepsilon_0 V}}d\sqrt{n_{ph}+1}$$

where $\vec{d}$ is the molecular transition dipole moment of the two-level oscillator, $\hbar\omega$ is the SPP resonance energy, ε_0 is the vacuum permittivity, V is the modal volume and n_{ph} refers to the number of photons in the system. Importantly, energy splitting can still exist even under zero photon conditions, that is n_{ph} = 0. This is indeed known as vacuum Rabi splitting ($\hbar\Omega_{VRS}$), attributed to electromagnetic vacuum fluctuations. In particular, quantum theory predicts that $\hbar\Omega_{VRS}$ is proportional to the square root of the absorbance which, in turn, is proportional to the concentration $\sqrt{N/V}$,[4,8] where N is the number of oscillators in the modal volume V. Hence, increasing the molecule concentration, namely confining the molecules into a smaller volume, is an effective way to increase the coupling strength.

In recent years there has been a great deal of effort towards understanding the dynamics of strongly coupled systems by transient spectroscopy experiments.[22,26–30] It has been demonstrated that the lifetime of the upper hybrid band in exciton–SPP systems can be much longer than the life of bare excited molecules. It was suggested that this result can be caused by a trap state observed in the upper band[26,28] or by the blockage of the vibrational relaxation modes due to the large Rabi splitting.[31–34] In this work, we report a comprehensive spectroscopic study of a prototypical SPP–molecule hybrid structure consisting of a gold nanoholes array coated with different constructions of J-aggregate molecules. The dynamics of the aforementioned system is revealed by an ultrafast pump–probe approach under resonant excitation. We demonstrate that the upper hybrid band shows a reduced lifetime upon increasing of the coupling strength.

Sample fabrication

The samples were fabricated through the deposition of 200 nm of gold on a CaF_2 substrate followed by the milling of the holes array by focused ion beams (FEI/Helios Nanolab 650). The total patterned area is 200 × 200 μm^2. The ratio between the periodicity and the hole diameter was kept at 2.5 while the period was varied from 260 to 360 nm. Afterwards, the samples were coated with a 300 nm thick layer of J-aggregate molecules, previously dispersed in liquid PVA (polyvinyl alcohol) with five different concentrations (from 0.5 to 4 mg mL^{-1}). To determine the absorbance of the J-aggregate film, samples with no gold layer were fabricated; the corresponding absorbance spectra are shown in Fig. 1 together with the scheme of the overall structure. The dye used in the experiments was 3,3′-disulfopropy1-5,5′-dichloro-9-ethylthia-carbocyanine triethylammonium salt (Thia; Hayashibara Biochemical Laboratories, Inc.), which has a sharp absorbance at 623 nm due to its large transition dipole moment upon J-aggregation. Such a feature is particularly suitable to achieve strong coupling with SPPs. In order to prevent oxidization, the samples were sealed by a glass slide under a nitrogen environment in a glove box with an oxygen concentration lower than 0.1 ppm.

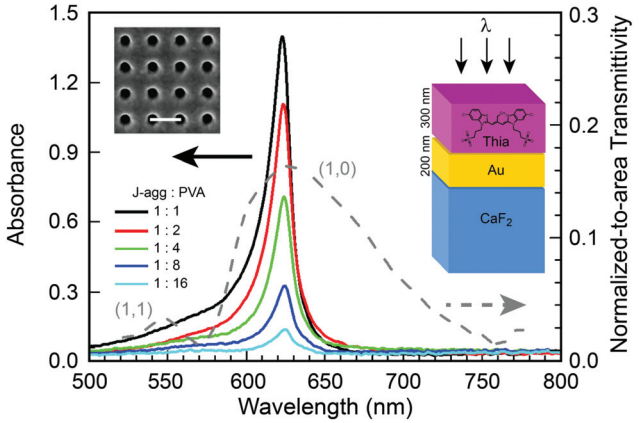

Fig. 1 Experimental absorbance spectra, at different concentrations of J-aggregate molecules, dispersed inside a 300 nm thick PVA film (solid lines). Normalized-to-area transmission spectrum of a gold hole array (period = 310 nm, white bar in the SEM image) covered with a 300 nm thick PVA film showing the broad SPP feature (gray dashed line). The low and high wavelength peaks correspond to the SPP orders (1,1) and (1,0), respectively. Inset: SEM image of the nano-patterned gold layer. Light is impinging from the top with normal incidence.

Numerical simulations

The numerical simulations were based on the Rigorous Coupled Wave Analysis (RCWA) method.[35] This numerical approach uses the concept of a unit cell to handle both 2D and 3D periodic structures and is specifically tailored for multilayer structures. The unit cell definition can have arbitrary geometry and the index distribution can consist of both standard dielectric materials and dispersive/lossy materials such as metals. The electromagnetic input can be an incident plane wave with arbitrary direction and polarization. Various simulation results can be outputted including far field components such as absorption, reflection and transmission. In particular, the latter quantity was utilized for a straight comparison with the experimental data.

The gold permittivity was described following the model in Alabastri *et al.*,[36] while PVA and CaF_2 permittivities were taken equal to 2.25 and 2.045, respectively, for all the wavelength spectrum of interest. The J-aggregate permittivity is described by a Lorentz oscillator model with the main resonant energy at 1.99 eV, as reported by Wurtz *et al.*[37] In order to match the

short-wavelength tail of the experimental absorption spectra (see Fig. 1), we slightly modified this simple model by adding a second oscillator at 2.16 eV.

Finally, the impinging light was considered normal to the top surface with linear polarization directed along the shortest distance between two adjacent holes.

Static measurements

Periodic metallic hole arrays have the capability to convert impinging radiation into SPPs modes resulting in a remarkable field confinement at the metal surface. Owing to the periodic pattern of the array, the desired SPP mode can be chosen by tuning the period thus to match the absorbance peak of the J-aggregates. Upon normal incidence radiation, the transmission spectrum of the gold holes array with a period of 310 nm (gray dashed line) shows two peaks corresponding to the SPP orders (1,1) and (1,0).[38,39] As illustrated in Fig. 1, the (1,0) SPP mode overlaps the absorbance peaks of the J-aggregate molecules, shown at different concentrations, with the result of maximizing the coupling strength. In Fig. 2a are plotted the simulated normal incidence transmission spectra for a series of gold hole arrays, characterized by different periodicities, covered by a 300 nm thick J-aggregate/PVA film (the latter manifesting an absorbance of 1.40 at 623 nm, as shown in Fig. 1). Similarly, in Fig. 2b are illustrated the corresponding experiment. As can be observed, the original plasmon peak illustrated in Fig. 1 (gray dashed line) splits into two bands. In particular, in Fig. 2c and d (numerical simulations and experimental characterization, respectively) the dispersion of the two bands is plotted as functions of both the holes array period from 260 nm to 360 nm and absorbance, and the result shows the characteristic feature of strong coup-

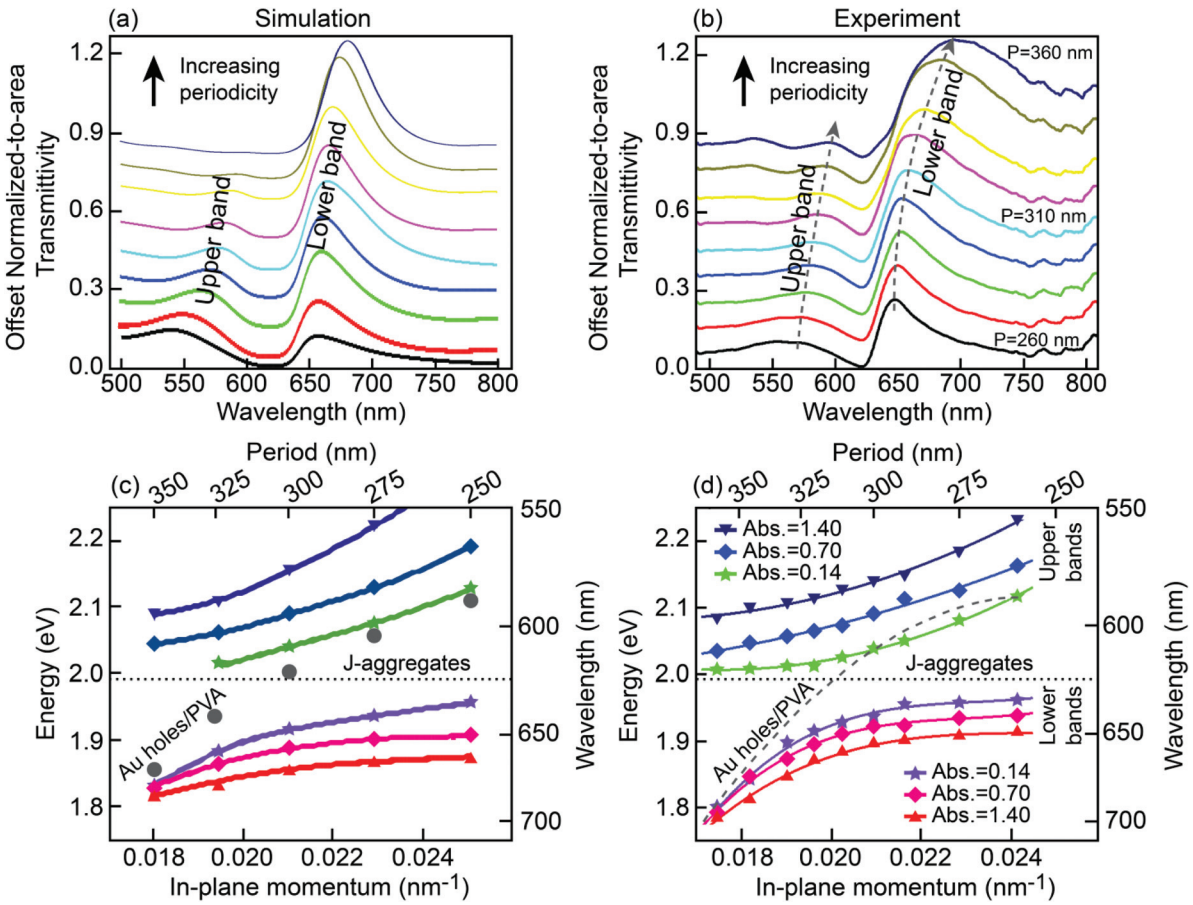

Fig. 2 (a) Simulated transmission spectra of a set of gold hole arrays (period from 250 nm to 350 nm as indicated by the arrow) covered by a 300 nm-thick PVA film doped with J-aggregates (chosen concentration such as the absorbance is 1.40 at 623 nm – see Fig. 1 black curve). (b) Experimental normalized-to-area transmission spectra of a set of gold hole arrays (period from 260 nm to 360 nm as indicated by the arrow) covered by a 300 nm-thick PVA film doped with J-aggregates (chosen concentration such as the absorbance is 1.40 at 623 nm – see Fig. 1 black curve). The two dashed lines highlight the shift of the lower and upper bands. (c) Simulated energy dispersion curves associated with three J-aggregate doped samples at different concentrations: 1.40 (blue and red triangles), 0.70 (light blue and pink squares) and 0.14 (green and violet stars). The gray dots represent the simulated dispersion curve for the J-aggregate-free (undoped) configuration. (d) Experimental energy dispersion curves corresponding to the undoped sample (no J-aggregate molecules, only gold holes array and PVA; gray dashed line) and to three different samples, doped with J-aggregates, showing absorbance of 1.40 (blue and red triangles), 0.70 (light blue and pink squares), and 0.14 (green and violet stars) calculated at 623 nm. These three values of absorbance were obtained by tuning the period of the holes array from 260 nm to 360 nm. The horizontal black dotted line corresponds to the J-aggregate 623 nm absorbance energy.

ling: the anticrossing of energies. An optimal Rabi splitting of 245 meV was experimentally measured at the resonance period of 310 nm for a concentration corresponding to an absorbance equal to 1.40. The dispersion curves for lower concentrations of J-aggregates are also represented in the figures. The decrease of the energy splitting magnitude upon lowering the J-aggregate concentration is clearly shown. In particular, J-aggregate/PVA film absorbances of 0.70 and 0.14 correspond to Rabi splitting of 161 meV and 99 meV, respectively.

In Fig. 3a and b, the former corresponding to simulations the latter to experiments, is highlighted the behaviour of Rabi splitting as a function of the absorbance for the resonant period of 310 nm and under normal incident radiation. A remarkable match is noticed between the two figures. The observed Rabi splitting displays a linear dependence on the square root of the J-aggregate absorbance (Fig. 3c simulations, Fig. 3d experiment) which, in turn, depends on the molecule concentration. Thus, the Rabi splitting observed in the normal transmission spectrum follows a $\sqrt{N/V}$ dependence, which is consistent with previous experimental results and the quantum theory description of strong coupling.[8,19] Above all, static measurements have clearly indicated that the hybrid system is in a strong coupling regime. To gain further insight into the corresponding dynamics of such a hybrid system with different coupling strengths, extensive studies were focused on transient absorption spectroscopy.

Transient absorption experiments

Femto-second transient absorption (TA) spectroscopy was carried out with a 100 fs laser pump–probe setup[40–42] based on a mode-locked Ti:sapphire laser/amplifier system (Solstice, Spectra-Physics). The amplified output from the regenerative amplifier (RGA, Spitfire, Spectra Physics), showing a 250 Hz repetition rate with a pulse energy of 1.5 mJ, 100 fs pulse width and 800 nm wavelength, was split into two parts. The strongest signal was used to generate the desired excitation pulse at 560 nm through a TOPAS system; the weakest part was focused on a sapphire substrate to generate a broadband white

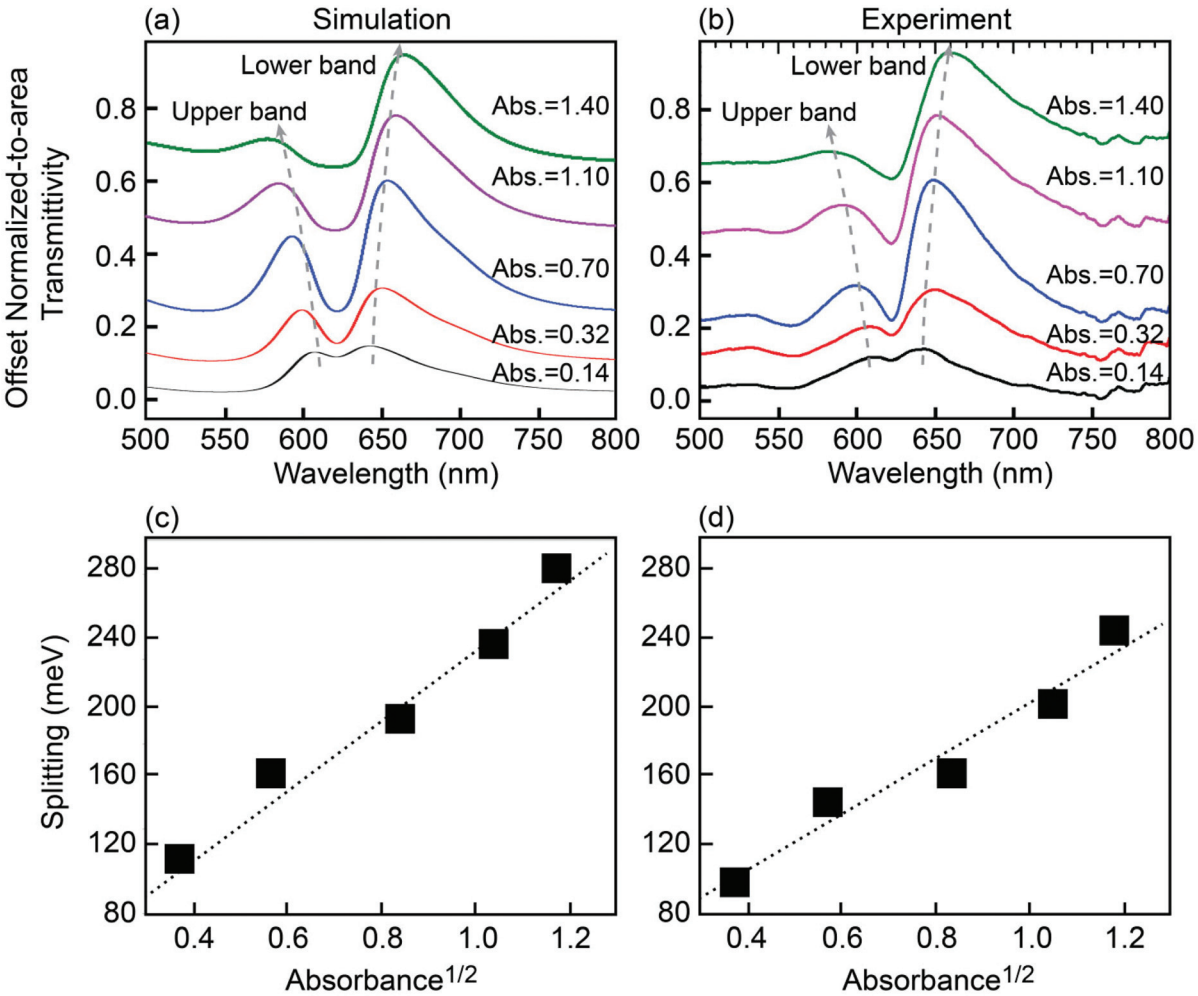

Fig. 3 (a) Simulated transmission spectra of gold holes array (period = 310 nm) upon increasing of the J-aggregate concentration (absorbance from 0.14 to 1.40 calculated at 623 nm). (b) Experimental characterization as in (a). (c) Simulated Rabi splitting values as a function of the square root of the J-aggregate molecule absorbance. The chosen period is 310 nm. (d) Corresponding experimental Rabi splitting.

light, from 450–800 nm, used as probe pulses. The two beams were orthogonally and collinearly recombined by a dichroic mirror, and focused on the sample at normal incidence through a microscope objective (NA 0.75, magnification 10). Of particular note is that, due to the chromatic aberrations, the focal planes of the pump and probe beams are indeed different. In this regard we had to apply a procedure to optimize the focusing of the probe beam. Otherwise, the pump would be out of focus thus providing a spatially uniform excitation pulse larger than the probed area. Finally, the reflected light from the sample was collected by the same objective and, by blocking the excitation light through a filter, the transient absorption data were collected by using a fibre-coupled sensitive spectrometer (Avantes AvaSpec-2048 × 14). The detection window was from 575 nm to 800 nm due to the blockage of the probe light by the dichroic mirror. To be noted is that the group velocity dispersion of the transient spectra was compensated by a chirp program.

In TA experiments we measured the variation of the optical density ΔOD, here defined as $-\log(R_{\mathrm{pump,probe}}/R_{\mathrm{probe}})$, where $R_{\mathrm{pump,probe}}$ is the reflection of the probe laser right after the pump signal has hit the sample, namely the sample reflection upon perturbation induced by the pump laser. Similarly, the R_{probe} describes the probe reflectivity under conditions far from the pump excitation. The three highest J-aggregate concentration samples, with absorbance values of 1.40, 1.10 and 0.70 calculated at 623 nm, were chosen for TA measurements. In Fig. 4a is shown the response of the reference sample, formed by J-aggregate/PVA spin-coated on a flat gold film, irradiated with a 560 nm laser pulse (upper band excitation). The result is a positive signal around 610 nm, which is attributed to excited state absorption, while the narrow negative signal at 623 nm, which is consistent with the steady-state absorption spectrum of Fig. 1, corresponds to the ground state bleaching of J-aggregates. As can be seen in Fig. 4b, the normalized bleaching kinetics associated with the three aforementioned absorbance values show very similar behaviour, namely fast decay, with no apparent dependence on the J-aggregate concentration.

The next step was to perform TA experiments on hybrid systems formed by gold hole arrays (period = 310 nm) covered by a film of PVA and J-aggregates at different concentrations (thickness of the film around 300 nm). Similarly to the experiment shown in Fig. 4, the samples were pumped by a pulsed laser at 560 nm corresponding to the upper hybrid band excitation. However, with respect to the reference sample of Fig. 4, the transient absorption spectra of the hybrid system show totally different features. Indeed, in Fig. 5, all three transient spectra are characterized by two bleaching signals (to be noted that due to the limitation of the detection window only a small part of the upper bands can be clearly detected). Especially for the highest J-aggregate concentration sample (absorbance 1.40), the upper band undergoes a strong blue-shift pushing it almost out of the detection window due to the very large Rabi splitting. Regardless, clear evidence of the existence of lower and upper bands is provided by all the considered concentrations.

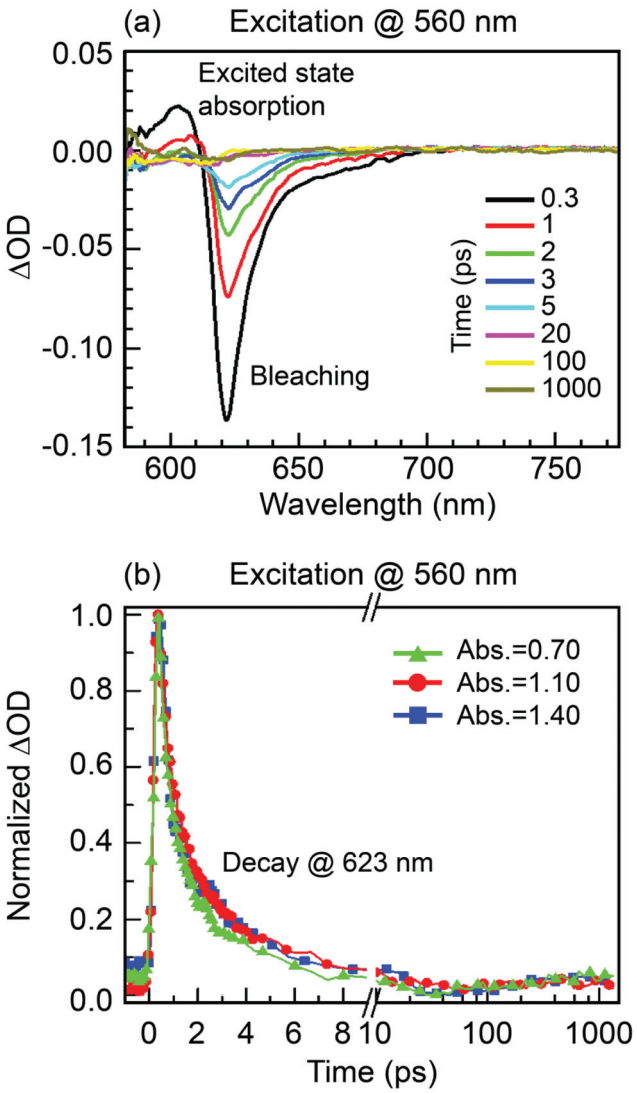

Fig. 4 (a) Transient absorption spectra of J-aggregates (absorbance of 1.10 at 623 nm) on a flat gold film. The spectra were recorded at 0.3, 1, 2, 3, 5, 20, 100 and 1000 ps. (b) Normalized bleaching dynamics of J-aggregates on a flat gold film at 623 nm with different concentrations (measured from reference samples with no gold layer). For both figures, a 560 nm excitation was considered (upper band excitation). ΔOD: optical density variation.

For J-aggregate concentrations with absorbance values of 1.10 and 1.40 (Fig. 5a and b), a positive signal associated with thermal effects[43] is observed between the two bleaching minima. Indeed, in the proposed configuration the resonant pump laser brings the system to an excited condition where the energy is shared and oscillates between the SPP modes associated with the gold nanoholes array and the excited state of J-aggregates. This leads to the hybrid states appearing in the TA spectra once the probe laser shines into the system. In the first moments, after the pump laser hits the sample (<1 ps), the system undergoes dephasing of the SPP resonances, namely the excited electrons tend to thermalize *via* electron–electron scattering. This phenomenon determines the creation

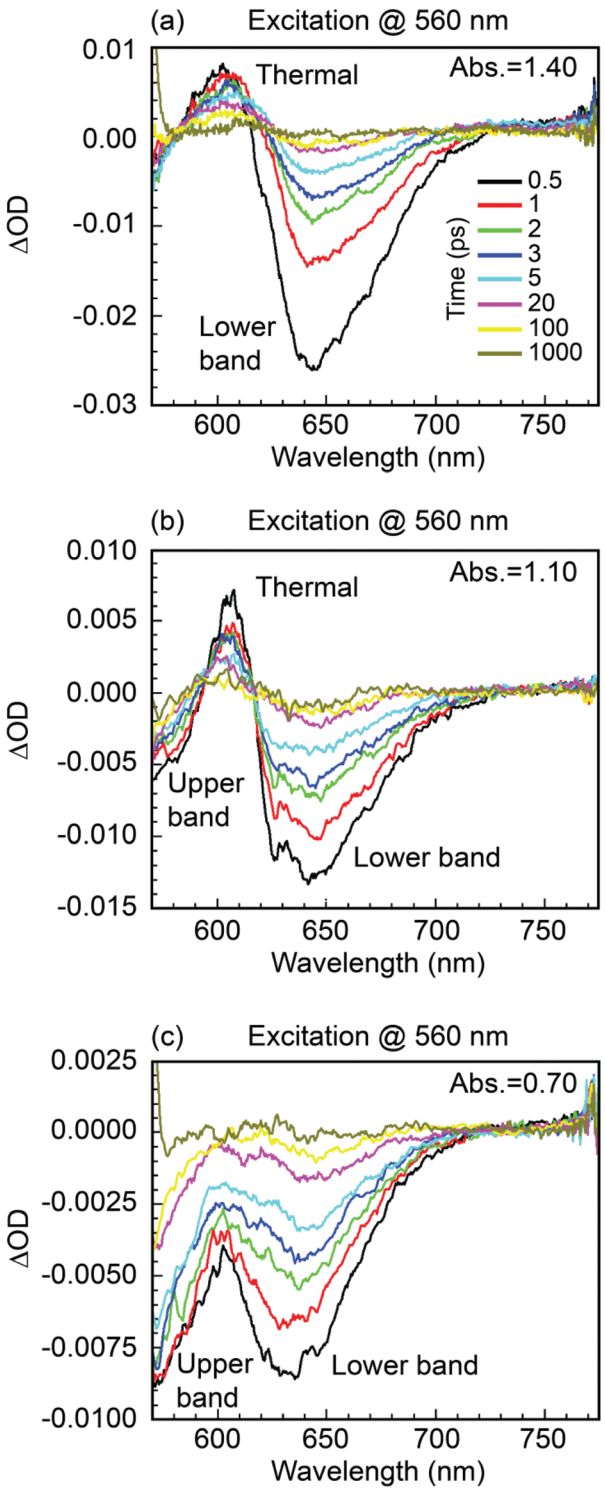

Fig. 5 Transient absorption spectra of PVA/J-aggregates with different concentrations ((a), (b), (c) corresponding to absorbance of 1.40, 1.10 and 0.70, respectively) deposited on a gold holes array under 560 nm excitation. The period of the array is taken to be equal to 310 nm. The PVA thickness is around 300 nm. The spectra were recorded at 0.5, 1, 2, 3, 5, 20, 100 and 1000 ps. ΔOD: optical density variation.

of new energy levels which will contribute to the absorption of probe photons, namely the transmission of the probe pulse is reduced with respect to the initial completely coherent (before dephasing) coupled hybrid system. In turn, this means a positive peak in the TA measurements.

However, by considering the amplitude of the thermal peak with respect to the overall spectra, we can argue that at these concentrations the hybrid system is probably dominated by a SPP-related non-thermal process. With the J-aggregate concentration decrease, the lower and upper bands gradually overlap with each other due to the Rabi splitting decrease (Fig. 5c); meanwhile the small positive signal submerges in the bleaching signals. Hence, for all the three samples under resonant 560 nm excitation, the dynamics of the hybrid systems is dominated by a SPP-related non-thermal process, in which the photophysics nature of strong coupling can be directly reflected.

In order to highlight the shift associated with different J-aggregate concentrations, the spectra recorded at 0.5 ps are shown in Fig. 6 for all three concentrations. The observed shift of the lower band (the upper band falls outside the detection window) confirms that the Rabi splitting increases with the J-aggregate concentration. This result is consistent with the static measurements shown in Fig. 3a.

The kinetics of the lower (Fig. 7a) and upper (Fig. 7b) hybrid bands with different coupling strengths (*i.e.* J-aggregate concentration) are compared with the kinetics of J-aggregates on a flat gold film and a flat glass substrate. The choice of materials is dictated by the need for ruling out any kind of strong coupling which might also occur between J-aggregates and a flat gold film. In particular, due to the detection window limitations, the upper band of the highest J-aggregate concentration sample (absorbance 1.40) cannot be detected. For the

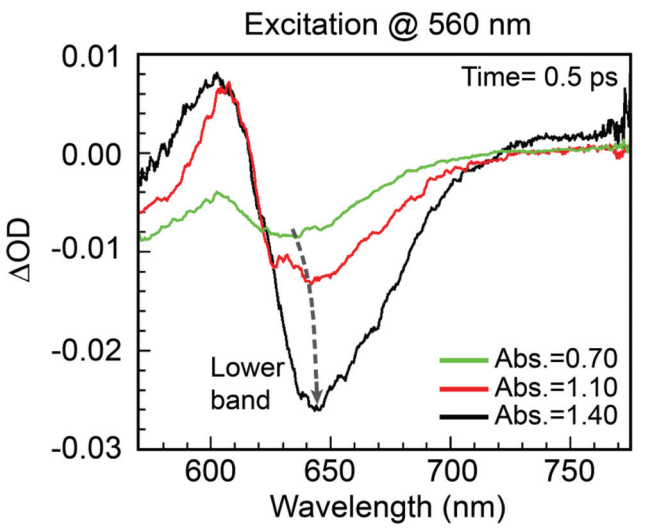

Fig. 6 Transient absorption spectra recorded at 0.5 ps for PVA/J-aggregates deposited on a gold holes array with period equal to 310 nm. Three different concentrations are considered. The lower band red shift is highlighted by the gray dashed line. Excitation: 560 nm. ΔOD: optical density variation.

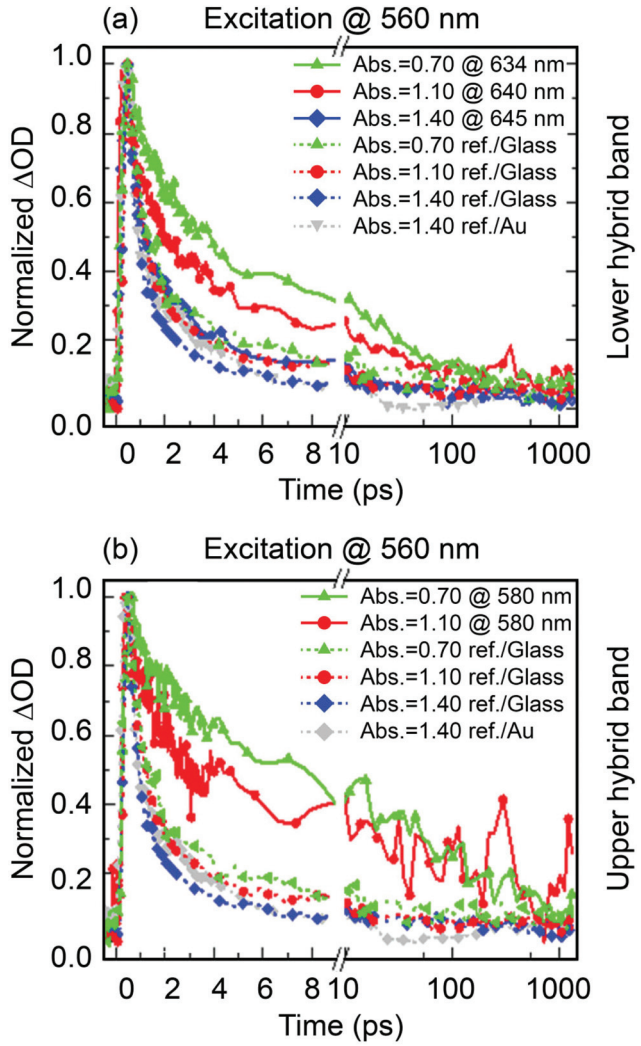

Fig. 7 Comparison between normalized bleaching dynamics of PVA/J-aggregates with different concentrations on gold hole arrays. (a) Lower hybrid bands, (b) upper hybrid bands measured at the detection window edge (580 nm). The normalized bleaching dynamics of PVA/J-aggregates (absorbance 1.40) on a flat gold film at 623 nm is shown as reference (gray dot line). Similarly, the figures also show the normalized bleaching dynamics of PVA/J-aggregates on a glass substrate with different concentrations (color dot lines). The excitation source is equal to 560 nm. ΔOD: optical density variation.

other two samples (absorbance 0.70 and 1.10) the kinetics of the upper bands are taken at the detection window edge, namely 580 nm. The results clearly show that the hybrid bands have longer lifetimes than the bleaching recovery of J-aggregates on flat gold films and glass substrates. Furthermore, Fig. 7 also shows that the kinetics of the hybrid exciton–SPP state is significantly affected by the J-aggregate concentration, namely the coupling strength. Indeed, the lifetime of both hybrid bands is reduced by increasing the coupling strength (higher J-aggregate concentration). This result is of particular interest especially when compared to the behaviour of J-aggregates on a flat gold film where no dependence on the concentration was detected, as shown in Fig. 4b (similar considerations also apply to J-aggregates on the glass substrate, see Fig. 7). This behaviour can be explained by taking into account the phonon bottleneck effect, the phenomenon responsible for suppressing vibrational relaxation levels, as already demonstrated in semiconductor quantum dots[44] and also demonstrated in strongly coupled hybrid systems as a result of the large Rabi splitting.[33] Indeed, under pump laser excitation the population density of plexitons (*i.e.* combination of plasmons and excitons) in hybrid bands increases with the concentration of J-aggregates (the amplitude of the bleaching signal is proportional to the J-aggregate concentration). With high population density, the interaction among plexitons is expected to be especially significant, which in turn means that energy is released to build up the population of phonons associated with different energies. These new energy levels will then represent a channel for a relaxation from the upper to the lower hybrid band and further to the ground state (namely removal of the bottleneck effect). Such behaviour is consistent with the bottleneck suppression found at high pump powers,[45] in which a higher population density can be created. Thus we suggest that the bottleneck relaxation mechanism can also play an important role in the dynamics of SPP-related systems and is strongly suppressed in hybrid structures with large Rabi splitting values (*i.e.* high dye concentration). This explains why the lifetime under high dye concentration approaches (*i.e.* shorten) the behaviour of the dye on top of a flat metal layer or glass substrate.

Conclusions

We have shown that strong coupling can occur between J-aggregate molecules and SPPs supported by gold nanohole arrays. We have investigated the dynamics of the formed hybrid state with different coupling strengths by using a femto-second pump–probe approach. Under upper band resonant excitation, two distinctive bleaching bands appeared in the transient absorption spectra showing an increased Rabi splitting upon increase of the concentration of J-aggregate molecules. This result was indeed confirmed by static measurements. Furthermore, the non-thermal kinetics of the hybrid state indicates that the upper band has an intrinsic long lifetime that depends on the Rabi splitting values as well. Our measurements suggest that the phonon bottleneck relaxation mechanism might play an important role in SPP-related dynamics processes. With stronger coupling strength, the bottleneck effect is suppressed, leading to a shorter lifetime of the upper hybrid band. This indicates that the coupling strength alters the dynamics of the hybrid system and offers new insights into the intrinsic photophysics of strong coupling.

Acknowledgements

The authors would like to recognize the financial support from the 3315 Innovative Teams Program of Ningbo – China; from

the European Research Council under the European Union's Seventh Framework Program (FP/2007-2013)/ERC Grant Agreement no. [616213]; from the National Science Foundation (awards no. 1102301 and 1254934); from the National Basic Research Program of China (973 Program, grant no. 2014CB921300), Natural Science Foundation China (NSFC) under grant no. 21273096 and no. 21473077 and from the Doctoral Fund Ministry of Education of China under grant no. 20130061110048.

Notes and references

1 S. Panaro, A. Nazir, C. Liberale, G. Das, H. Wang, F. De Angelis, R. Proietti Zaccaria, E. Di Fabrizio and A. Toma, *ACS Photonics*, 2014, **1**, 310–314.
2 J. Song, R. Proietti Zaccaria, M. B. Yu and X. W. Sun, *Opt. Express*, 2006, **14**, 8812–8826.
3 A. Salomon, S. Wang, J. A. Hutchison, C. Genet and T. W. Ebbesen, *ChemPhysChem*, 2013, **14**, 1882–1886.
4 A. González-Tudela, P. A. Huidobro, L. Martín-Moreno, C. Tejedor and F. J. García-Vidal, *Phys. Rev. Lett.*, 2013, **110**, 126801.
5 Y.-W. Hao, H.-Y. Wang, Y. Jiang, Q.-D. Chen, K. Ueno, W.-Q. Wang, H. Misawa and H.-B. Sun, *Angew. Chem., Int. Ed.*, 2011, **123**, 7970–7974.
6 J. Bellessa, C. Symonds, K. Vynck, A. Lemaitre, A. Brioude, L. Beaur, J. C. Plenet, P. Viste, D. Felbacq, E. Cambril and P. Valvin, *Phys. Rev. B: Condens. Matter*, 2009, **80**, 033303.
7 Y. Sugawara, T. A. Kelf, J. J. Baumberg, M. E. Abdelsalam and P. N. Bartlett, *Phys. Rev. Lett.*, 2006, **97**, 266808.
8 J. Dintinger, S. Klein, F. Bustos, W. L. Barnes and T. W. Ebbesen, *Phys. Rev. B: Condens. Matter*, 2005, **71**, 035424.
9 Y.-F. Zhang, D.-J. Yang, J.-H. Wang, Y.-L. Wang, S.-J. Ding, L. Zhou, Z.-H. Hao and Q.-Q. Wang, *Nanoscale*, 2015, **7**, 8503–8509.
10 S. Wang, T. Chervy, J. George, J. A. Hutchison, C. Genet and T. W. Ebbesen, *J. Phys. Chem. Lett.*, 2014, **5**, 1433–1439.
11 R. Bose, T. Cai, K. R. Choudhury, G. S. Solomon and E. Waks, *Nat. Photonics*, 2014, **8**, 858–864.
12 A. Canaguier-Durand, E. Devaux, J. George, Y. Pang, J. A. Hutchison, T. Schwartz, C. Genet, N. Wilhelms, J.-M. Lehn and T. W. Ebbesen, *Angew. Chem., Int. Ed.*, 2013, **52**, 10533–10536.
13 T. Schwartz, J. A. Hutchison, C. Genet and T. W. Ebbesen, *Phys. Rev. Lett.*, 2011, **106**, 196405.
14 Y.-Y. Lai, Y.-P. Lan and T.-C. Lu, *Light: Sci. Appl.*, 2013, **2**, e76.
15 S. Chen, G. Li, D. Lei and K. W. Cheah, *Nanoscale*, 2013, **5**, 9129–9133.
16 W. Wang, P. Vasa, R. Pomraenke, R. Vogelgesang, A. De Sio, E. Sommer, M. Maiuri, C. Manzoni, G. Cerullo and C. Lienau, *ACS Nano*, 2014, **8**, 1056–1064.
17 S. Gambino, M. Mazzeo, A. Genco, O. Di Stefano, S. Savasta, S. Patanè, D. Ballarini, F. Mangione, G. Lerario, D. Sanvitto and G. Gigli, *ACS Photonics*, 2014, **1**, 1042–1048.
18 S. Kéna-Cohen, S. A. Maier and D. D. C. Bradley, *Adv. Opt. Mater.*, 2013, **1**, 827–833.
19 J. A. Hutchison, T. Schwartz, C. Genet, E. Devaux and T. W. Ebbesen, *Angew. Chem., Int. Ed.*, 2012, **51**, 1592–1596.
20 J. A. Hutchison, A. Liscio, T. Schwartz, A. Canaguier-Durand, C. Genet, V. Palermo, P. Samorì and T. W. Ebbesen, *Adv. Mater.*, 2013, **25**, 2481–2485.
21 J. D. Plumhof, T. Stöferle, L. Mai, U. Scherf and R. F. Mahrt, *Nat. Mater.*, 2014, **13**, 247–252.
22 P. Vasa, W. Wang, R. Pomraenke, M. Lammers, M. Maiuri, C. Manzoni, G. Cerullo and C. Lienau, *Nat. Photonics*, 2013, **7**, 128–132.
23 K. S. Daskalakis, S. A. Maier, R. Murray and S. Kéna-Cohen, *Nat. Mater.*, 2014, **13**, 271–278.
24 K. F. MacDonald, Z. L. Samson, M. I. Stockman and N. I. Zheludev, *Nat. Photonics*, 2009, **3**, 55–58.
25 P. Törmä and W. L. Barnes, *Rep. Prog. Phys.*, 2015, **78**, 013901.
26 S. Balci, C. Kocabas, B. Küçüköz, A. Karatay, E. Akhüseyin, H. Gul Yaglioglu and A. Elmali, *Appl. Phys. Lett.*, 2014, **105**, 051105.
27 T. Virgili, D. Coles, A. M. Adawi, C. Clark, P. Michetti, S. K. Rajendran, D. Brida, D. Polli, G. Cerullo and D. G. Lidzey, *Phys. Rev. B: Condens. Matter*, 2011, **83**, 245309.
28 N. T. Fofang, N. K. Grady, Z. Fan, A. O. Govorov and N. J. Halas, *Nano Lett.*, 2011, **11**, 1556–1560.
29 P. Vasa, R. Pomraenke, G. Cirmi, E. De Re, W. Wang, S. Schwieger, D. Leipold, E. Runge, G. Cerullo and C. Lienau, *ACS Nano*, 2010, **4**, 7559–7565.
30 A. Salomon, C. Genet and T. W. Ebbesen, *Angew. Chem., Int. Ed.*, 2009, **121**, 8904–8907.
31 T. Schwartz, J. A. Hutchison, J. Léonard, C. Genet, S. Haacke and T. W. Ebbesen, *ChemPhysChem*, 2013, **14**, 125–131.
32 D. M. Coles, P. Michetti, C. Clark, W. C. Tsoi, A. M. Adawi, J.-S. Kim and D. G. Lidzey, *Adv. Funct. Mater.*, 2011, **21**, 3691–3696.
33 D. M. Coles, R. T. Grant, D. G. Lidzey, C. Clark and P. G. Lagoudakis, *Phys. Rev. B: Condens. Matter*, 2013, **88**, 121303.
34 L. Mazza, S. Kéna-Cohen, P. Michetti and G. C. La Rocca, *Phys. Rev. B: Condens. Matter*, 2013, **88**, 075321.
35 R. Proietti Zaccaria, *Opt. Laser Eng.*, 2016, **76**, 70–73.
36 A. Alabastri, S. Tuccio, A. Giugni, A. Toma, C. Liberale, G. Das, F. Angelis, E. Fabrizio and R. Proietti Zaccaria, *Materials*, 2013, **6**, 4879.
37 G. A. Wurtz, P. R. Evans, W. Hendren, R. Atkinson, W. Dickson, R. J. Pollard, A. V. Zayats, W. Harrison and C. Bower, *Nano Lett.*, 2007, **7**, 1297–1303.

38 Y. Nishijima, Y. Adachi, L. Rosa and S. Juodkazis, *Opt. Mater. Express*, 2013, **3**, 968–976.
39 Y. Nishijima, H. Nigorinuma, L. Rosa and S. Juodkazis, *Opt. Mater. Express*, 2012, **2**, 1367–1377.
40 H. Wang, H.-Y. Wang, B.-R. Gao, Y. Jiang, Z.-Y. Yang, Y.-W. Hao, Q.-D. Chen, X.-B. Du and H.-B. Sun, *Appl. Phys. Lett.*, 2011, **98**, 251501.
41 H. Wang, H.-Y. Wang, B.-R. Gao, L. Wang, Z.-Y. Yang, X.-B. Du, Q.-D. Chen, J.-F. Song and H.-B. Sun, *Nanoscale*, 2011, **3**, 2280–2285.
42 L. Wang, C.-F. Wu, H.-Y. Wang, Y.-F. Wang, Q.-D. Chen, W. Han, W.-P. Qin, J. McNeill and H.-B. Sun, *Nanoscale*, 2013, **5**, 7265–7270.
43 G. V. Hartland, *Chem. Rev.*, 2011, **111**, 3858–3887.
44 J. Urayama, T. B. Norris, J. Singh and P. Bhattacharya, *Phys. Rev. Lett.*, 2001, **86**, 4930–4933.
45 A. I. Tartakovskii, M. Emam-Ismail, R. M. Stevenson, M. S. Skolnick, V. N. Astratov, D. M. Whittaker, J. J. Baumberg and J. S. Roberts, *Phys. Rev. B: Condens. Matter*, 2000, **62**, R2283–R2286.